

DeblurDiNAT: A Lightweight and Effective Transformer for Image Deblurring

Hanzhou Liu¹, Bingham Li¹, Chengkai Liu¹, and Mi Lu¹

Texas A&M University, College Station TX 77843, USA
{hanzhou1996, lbh1994usa, liuchengkai}@tamu.edu
mlu@ece.tamu.edu

Abstract. Blurry images may contain local and global non-uniform artifacts, which complicate the deblurring process and make it more challenging to achieve satisfactory results. Recently, Transformers generate improved deblurring outcomes than existing CNN architectures. However, the large model size and long inference time are still two bothersome issues which have not been fully explored. To this end, we propose DeblurDiNAT, a compact encoder-decoder Transformer which efficiently restores clean images from real-world blurry ones. We adopt an alternating dilation factor structure with the aim of global-local feature learning. Also, we observe that simply using self-attention layers in networks does not always produce good deblurred results. To solve this problem, we propose a channel modulation self-attention (CMSA) block, where a cross-channel learner (CCL) is utilized to capture channel relationships. In addition, we present a divide and multiply feed-forward network (DMFN) allowing fast feature propagation. Moreover, we design a lightweight gated feature fusion (LGFF) module, which performs controlled feature merging. Comprehensive experimental results show that the proposed model, named DeblurDiNAT, provides a favorable performance boost without introducing noticeable computational costs over the baseline, and achieves state-of-the-art (SOTA) performance on several image deblurring datasets. Compared to nearest competitors, our space-efficient and time-saving method demonstrates a stronger generalization ability with 3%-68% fewer parameters and produces deblurred images that are visually closer to the ground truth. The source code and pre-trained models are available at <https://github.com/HanzhouLiu/DeblurDiNAT>.git.

1 Introduction

Vision systems are widely applied to autonomous driving, medical research, and manufacturing [26]. It is essential to use high-quality sensing devices to capture clear visual data for them. Blurry photos are still unavoidable although camera modules develop fast [39]. Image deblurring is the procedure of removing blur artifacts from unclear or blurry images [4, 44], and is traditionally conceptualized as an inverse filtering problem [2, 12, 31]. Non-deep learning methods exhibit robust efficacy in certain scenarios [1, 3, 17, 43]. However, their performance is

suboptimal in more intricate yet prevalent cases, for example, those involving strong motion blur [50].

In the past decade, convolutional neural networks (CNN) play an important role in computer vision tasks [7, 27, 49]. The significant strength of CNNs is their ability to acquire generalizable image priors from large-scale datasets, making them become de facto for image deblurring [5, 10, 21, 24, 29, 34, 38, 51]. Nonetheless, the limited receptive field constrained by the kernel size and network depth prevents CNNs from modeling long-range pixel dependencies.

Transformers, initially designed for natural language processing (NLP) [41], have adapted to handle visual data, challenging the dominance of CNNs in computer vision [9, 22, 30, 46]. Self-attention (SA), a fundamental component in Transformers, differs from the convolutional layer in CNNs and facilitates long-range feature learning through scaled dot-product. This attribute hinders the capacity of Transformers in capturing local blurred patterns, which frequently exist in real-world blurry images [12, 13, 40]. Also, the computational costs increase quadratically to process high-resolution images. To overcome these limitations, most methods divide image data into small spatial windows or strips. Although the model complexity is reduced and short-range blurring information is learnt, the deblurring performance may be negatively impacted due to the loss of spatial information. It has proven to be a challenging task for deblurring Transformers [23, 40, 42, 47] to achieve the optimal equilibrium between efficacy and efficiency.

In this paper, we intend to find a balance that ensures optimized computation while maintaining high deblurring performance. For that purpose, we propose DeblurDiNAT, an effective and efficient deblurring Transformer, built on a novel hybrid encoder-decoder architecture. DeblurDiNAT produces high-quality deblurred images and shows a strong generalization ability, with compact size and fast inference time. Our SA strategy is based on Dilated Neighborhood Attention (DiNA) [14], a flexible and powerful sparse global attention pattern. DiNA introduces a dilation factor to allow controllable receptive fields without additional overhead [14, 15]. Similar to dilated convolutions [45], the dilation factor in DiNA indicates how much the kernel is widened, and a larger dilation factor results in a larger receptive field [20]. Through stacking Transformer blocks with small and large dilation factors alternately, our network learns both global and local blur information in an efficient way. To the best of our knowledge, this paper is the first work that comprehensively investigates the potential of DiNA in an image restoration task.

We propose a new SA scheme, channel modulation self-attention (CMSA), addressing a critical issue of applying SA to image data, *i.e.*, SA lacking the ability to model cross-channel relationships effectively. CMSA uses element-wise multiplications to merge feature maps that are separately learnt by a dilated neighborhood attention block and a cross-channel learner (CCL). CCL draws inspiration from the channel attention method in SENet [19]. The significant difference is that rather than fully connecting all channels, CCL only considers each channel’s nearest neighbors, which is intuitively consistent with the ratio-

nale of neighborhood attention. We thoroughly compare our parallel design to variants with CCL at different positions.

The other basic component of Transformers is the feed-forward network (FN). There are two common types of FNs in SOTA deblurring Transformers, FNs composed of fully connected layers followed by activation layers [40, 42], and the ones based on convolutional layers [23, 47]. In this paper, we aim to investigate and optimize the second type, where a non-linear GELU [16] function is used as part of gating mechanisms for controlled feature propagation. However, questions may arise regarding the effectiveness of GELU in this structure and none of them [23, 47] provide experimental data to analyze its impacts on deblurring performance. In this paper, we propose a divide and multiply feed-forward network (DMFN) without any non-linear activation function, thereby reducing computational loads. Experimental results show that this simple and clean design positively influences the overall deblurring outcomes.

Apart from the above modules, we visit a different element of the network, feature fusion, to further boost the deblurring power of our lightweight Transformer. We make the following empirical observations. Firstly, the conventional concatenate and convolve method may be a bottleneck of deblurring models. Secondly, existing SOTA feature fusion approaches [6, 28], originally designed for CNNs, add extra computational complexity to Transformers due to unneeded convolution, activation and normalization. Thirdly, in fusion blocks, positive impacts of SA are negligible. Motivated by the above observations, we present a lightweight gated feature fusion (LGFF) module for encoder-decoder Transformers, a universal method to merge multi-scale or same-scale features.

Our contributions in this work are summarized as follows:

- We propose DeblurDiNAT, a compact Transformer for image deblurring, capable of capturing both global and local blurred patterns.
- We present a channel modulation self-attention (CMSA) block, allowing the Transformer to learn complex multi-channel data in an efficient way.
- We develop a divide and multiply feed-forward network (DMFN), which propagates features with optimal computational costs.
- We design a lightweight gated feature fusion (LGFF) approach that is well-suited for both multi-scale and same-scale feature aggregation.
- Extensive experiments show that DeblurDiNAT not only achieves SOTA performance, but also ensures efficiency and robustness.

2 Background

CNN-based Image Deblurring Models Deep CNN-based methods have proven to be highly effective in image deblurring [5, 11, 18, 25, 32, 33, 37, 38, 48]. Tao *et al.* [38] investigated the coarse-to-fine scheme, and proposed a Scale-recurrent Network (SRN) with a simpler structure compared to conventional cascaded neural networks. Cho *et al.* [5] revisited the coarse-to-fine strategy and presented a multi-input multi-output UNet (MIMO-UNet) for fast image deblurring. Mehri *et al.* [32] chose to utilize multi-level representations and designed

a multi-stage progressive architecture (MPRNet) to significantly enhance the deblurring performance.

Transformer-based Image Deblurring Models Researchers have dedicated significant efforts to capturing spatial variant blur, in order to improve the applicability of Transformers in real-world image deblurring [23, 40, 42, 47]. Tsai *et al.* [40] leveraged intra-strip and inter-strip attention for estimating various blurred patterns and constructed Stripformer for dynamic scene image deblurring [40]. Kong *et al.* [23] advanced deblurring Transformers by introducing quantization and Fourier transform to self-attention and feed-forward networks. Although these approaches have produced better deblurring results than prevalent CNN models, they have not fully utilized cross-channel relationships in complex multi-channel data. Zamir *et al.* [47] proposed Restormer, an efficient Transformer which computes cross-covariance across feature channels rather than spatial dimension to model global connectivity. However, this architecture learns short-range dependencies exclusively through convolutional layers, which may fall short in effectively refining image details.

Multi-scale Feature Fusion Li *et al.* [28] presented a Gated Fully Fusion (GFF) mechanism using multiple addition gates and element-wise multiplications to generate high-level feature maps for semantic segmentation. Dong *et al.* [8] proposed a Dense Feature Fusion (DFF) module for U-Net architectures, based on the back-projection technique. Nevertheless, redundant matrix operations in GFF and stacked convolutional layers in DFF result in heavy computational burdens. Cho *et al.* [5] adopted Asymmetric Feature Fusion (AFF) composed of only two convolutional layers to allow fast information flow from various scales across a U-Net. While the AFF design is simple, it is a limiting factor for deblurring models to learn complex representations in heavily blurred image data.

3 Method

Existing deblurring Transformers struggle with complexity and accuracy trade-off. To achieve SOTA performance with minimal space and time costs, we propose a Transformer-based architecture, DeblurDiNAT, as an effective, efficient and robust deblurring model. We firstly introduce DiNA [14] to image deblurring and present an alternating dilation factor structure to capture global and local blurred patterns. Then, we detail the novel channel modulation self-attention (CMSA), a basic component of DeblurDiNAT, leveraging the channel relationships for enhanced deblurring performance. After that, we present an easy while effective feature propagation method, divide and multiply feed-forward network (DMFN). Lastly, we provide a lightweight gated feature fusion (LGFF) module to further reduce computational costs and improve performance, which is suitable for both multi-scale and single-scale feature fusion. Fig. 1 demonstrates

the overview of DeblurDiNAT architecture. Each encoder performs convolutions followed by Leaky ReLU activations, where convolutional layers capture spatial hierarchies in the input images and Leaky ReLU contributes to a robust learning process. Each decoder consists of cascaded Transformer blocks, in which global self-attention and local self-attention are adopted alternately to learn both long-range and short-range feature dependencies.

Most computational operations in Transformers come from self-attention (SA). The SA mechanism proposed in our work is an extension to Dilated Neighborhood Attention (DiNA) [14, 15]. DiNA serves as a flexible SA method for both local and global learning by adjusting the dilation factor without introducing additional complexity theoretically. For simplicity, consider a feature map $X \in \mathbb{R}^{n \times d}$, where n is the number of tokens (basic data units) and d is the dimension; the *query* and *key* linear projections of X , Q and K ; and relative positional biases between two tokens i and j , $B(i, j)$. Given a dilation factor δ and neighborhood size k , the attention weights for the i -th token is defined as:

$$\mathbf{A}_i^{(k, \delta)} = \begin{bmatrix} Q_i K_{\rho_1^\delta(i)}^T + B(i, \rho_1^\delta(i)) \\ Q_i K_{\rho_2^\delta(i)}^T + B(i, \rho_2^\delta(i)) \\ \vdots \\ Q_i K_{\rho_k^\delta(i)}^T + B(i, \rho_k^\delta(i)) \end{bmatrix}. \quad (1)$$

The corresponding matrix $\mathbf{V}_i^{(k, \delta)}$, whose elements are the i -th token's k adjacent *value* linear projections, can be obtained by:

$$\mathbf{V}_i^{(k, \delta)} = \left[V_{\rho_1^\delta(i)}^T \ V_{\rho_2^\delta(i)}^T \ \cdots \ V_{\rho_k^\delta(i)}^T \right]^T. \quad (2)$$

The output feature map of DiNA for the i -th token is achieved by:

$$DiNA_k^\delta(i) = \text{softmax}\left(\frac{\mathbf{A}_i^{(k, \delta)}}{\sqrt{d_k}}\right) \mathbf{V}_i^{(k, \delta)}. \quad (3)$$

We refer our readers to the original work for complexity analysis [15].

3.1 Alternating Dilation Factor Structure

In DiNA, the lower bound for the dilation factor is 1; the upper bound for the dilation factor is computed as $\lfloor \frac{n}{k} \rfloor$, the greatest integer less than or equal to $\frac{n}{k}$, where n is the feature size, and k is the kernel size. By incrementing the value of dilation factor, the self-attention window size is widened, which means longer-range dependencies are learnt by the network. To capture both local and global blurred patterns, we design a cascaded structure where the dilation factor $\delta \in \{1, \lfloor \frac{n}{k} \rfloor\}$ takes the lower bound value and upper bound value alternately. k is set to a constant number 7 in our design.

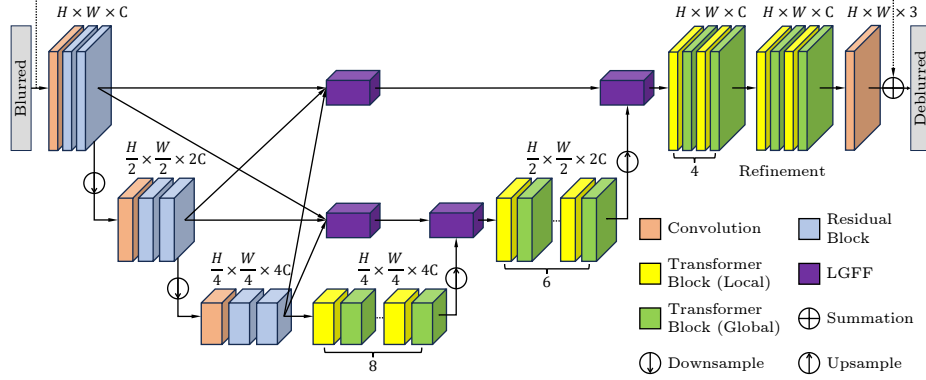


Fig. 1: Architecture of DeblurDiNAT for single image deblurring. DeblurDiNAT is a hybrid encoder-decoder network, where cascaded residual blocks extract multi-scale image features from input images, and alternating global and local Transformer blocks leverage hierarchical features for image reconstruction. Lightweight gated feature fusion (LGFF) modules perform effective and flexible feature fusion across the model.

3.2 Channel Modulation Self Attention

Channel Modulation Self Attention (CMSA) is proposed as a powerful Transformer component which not only learns the spatial relationships between pixels but also captures channel dependencies. Fig. 2 (b)-(d) show that our proposed CMSA is composed of two units, DiNA and a cross-channel learner (CCL). CCL is essentially a lightweight channel attention module, which adaptively tunes the output feature maps of the self-attention layer according to the normalized input data. To optimize the extra runtime caused by CCL, we place it parallel to DiNA, and our extensive experiments show that this parallel design outperforms other variants, which are discussed in Sec. 4.3.

Given a layer normalized tensor $X \in \mathbb{R}^{\hat{H} \times \hat{W} \times \hat{C}}$. The cross-channel learner (CCL) is computed as:

$$CCL(X) = f^{-1}(Conv_3(f(AAP_{2d}^{1 \times 1}(X)))), \quad (4)$$

where $AAP_{2d}^{1 \times 1}$ indicates a 2D adaptive average pooling, outputting a tensor of size 1×1 . f is a function which squeezes and transposes a $C \times 1 \times 1$ matrix, and results in a $1 \times C$ matrix. $Conv_3$ denotes a 1D convolution with a kernel size of 3. The batch dimension is ignored for simplicity in our discussions.

Then, the full process of CMSA is formulated as,

$$\hat{X} = DiNA(X) \odot CCL(X), \quad (5)$$

where \odot denotes element-wise multiplication; \hat{X} denotes the output tensor. $DiNA$ is illustrated in Eq. (1), Eq. (2), and Eq. (3).

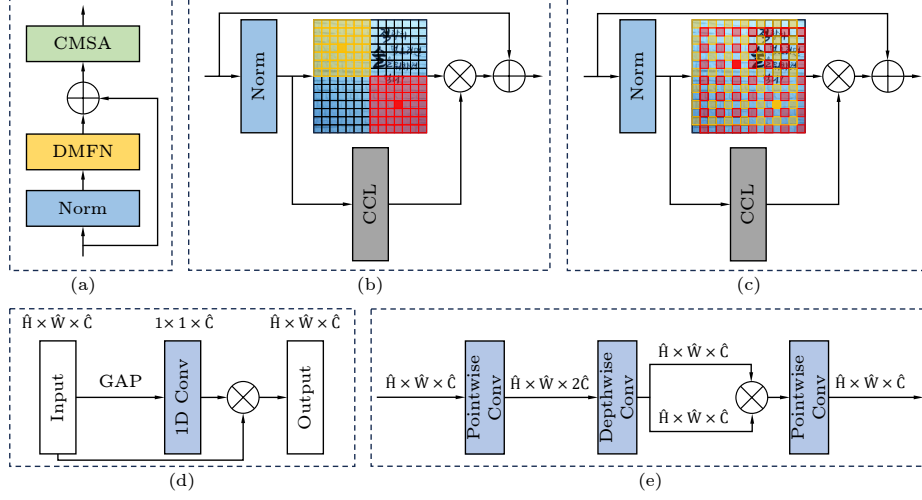


Fig. 2: The structures of (a) Transformer block, (b) local channel modulation self-attention (CMSA) with a dilation factor of 1, (c) global CMSA with a dilation factor of $\frac{n}{k}$, (d) cross-channel learner (CCL), and (e) divide and multiply feed-forward network (DMFN). The kernel sizes used in 1D Conv and Depthwise Conv are set to 3.

3.3 Divide and Multiply Feed-Forward Network

Our proposed DMFN, as shown in Fig. 2 (e), incorporates a 1×1 point-wise convolution layer followed by a 3×3 depth-wise separate convolution layer to explicitly model channel interactions in the features. Using depth-wise convolution is inspired by Restormer and FFTformer [23, 47], where GELU functions are also introduced as part of gating mechanisms for controlled information flow. We argue that this non-linear function not only increases computational costs, but also hinders the deblurring performance of Transformers. Our divide and multiply strategy is simple while effective. From a layer normalized feature $X \in \mathbb{R}^{\hat{H} \times \hat{W} \times \hat{C}}$, DMFN first applies point-wise convolutions to expand the feature channels by a factor $\gamma = 2$. After that, 3×3 depth-wise convolutions are utilized to aggregate spatial context, generating $X_0 \in \mathbb{R}^{\hat{H} \times \hat{W} \times 2\hat{C}}$. Next, we equally divide the intermediate feature map along the channel dimension, yielding X_1 and X_2 , so that their element-wise multiplication result is of shape $\mathbb{R}^{\hat{H} \times \hat{W} \times \hat{C}}$. The overall DMFN process is formulated as:

$$\begin{aligned} \hat{X} &= Conv_{1 \times 1}(DM(X)) + X, \\ DM(X) &= X_1 \odot X_2, \end{aligned} \quad (6)$$

where $Conv_{1 \times 1}$ denotes a convolution with filter size of 1×1 ; DM represents our divide and multiply strategy; X_1 and X_2 are the two equally divided feature maps of size $\mathbb{R}^{\hat{H} \times \hat{W} \times \hat{C}}$.

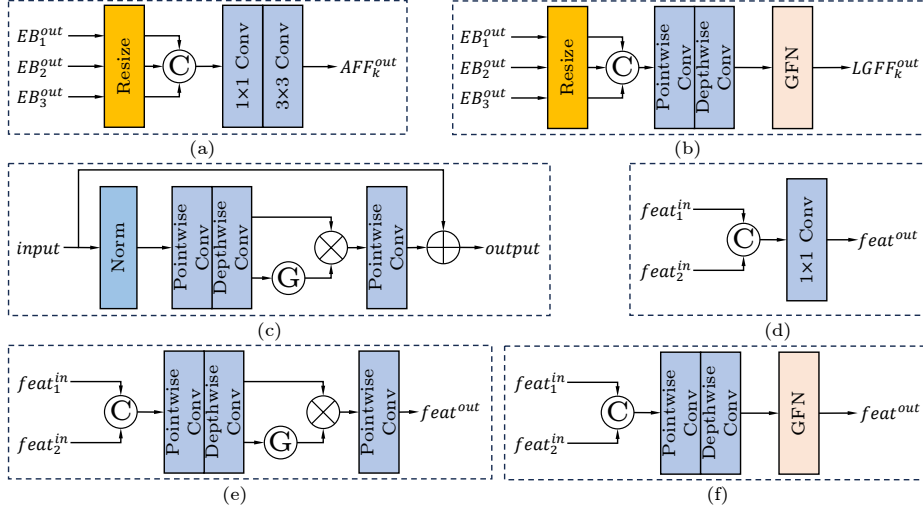


Fig. 3: The structures of (a) multi-scale AFF [5], (b) multi-scale LGFF, (c) gated feed-forward network (GFN), (d) same-scale simplified feature fusion (SFF), (e) same-scale simplified gated feature fusion (SGFF), (f) same-scale LGFF.

3.4 Lightweight Gated Feature Fusion

Most feature fusion methods in deblurring Transformers only aggregate same-scale data, which fail to exploit the full potential of feature hierarchies in images. We propose lightweight gated feature fusion (LGFF) that is also able to merge multi-scale features, illustrated in Fig. 3 (b)-(c). LGFF is formulated as:

$$\begin{aligned} LGFF_1^{out} &= LGFF_1(EB_1^{out}, (EB_2^{out})^{\times 2}, (EB_3^{out})^{\times 4}), \\ LGFF_2^{out} &= LGFF_2((EB_1^{out})^{\times \frac{1}{2}}, EB_2^{out}, (EB_3^{out})^{\times 2}), \end{aligned} \quad (7)$$

where $LGFF_i^{out}$ and EB_i^{out} denote the output features of the i -th LGFF and the i -th encoder block; $\times 2$ and $\times 4$ represents upscaling by 2 and 4; $\times \frac{1}{2}$ means downscaling by 2. When applying LGFF to same-scale features, the output is:

$$feature^{out} = LGFF(feature_1^{in}, feature_2^{in}), \quad (8)$$

where $feature_1^{in}$ and $feature_2^{in}$ are of the same shape. See Fig. 3 (f).

Different from the multi-scale asymmetric feature fusion (AFF) adopted in MIMO-Unet [5], we take advantage of depth-wise convolution and point-wise convolution to preprocess the concatenated features and reduce the number of channels. After that, a feed-forward network with two parallel paths is utilized to control the information flow across multiple depth levels.

4 Experiments and Analysis

4.1 Datasets and Implementation Details

The training dataset is GoPro [33] composed of 2103 blurred and clean image pairs for training and 1111 pairs for testing. We tested DeblurDiNAT on the two synthetic datasets GoPro [33] and HIDE [36], and evaluated deblurring methods on real-world datasets RealBlur-R [35] and RealBlur-J [35]. DeblurDiNAT was trained only on the GoPro [33] training dataset and directly applied to the GoPro [33], HIDE [36], RealBlur-R [35] and RealBlur-J [35] test datasets.

We propose DeblurDiNAT-S (Small) and DeblurDiNAT-L (Large), the two variants of our model. The number of Transformer blocks in DeblurDiNAT-S are [4, 6, 8] at each level, attention heads are [2, 4, 8], and the number of channels are [64, 128, 256]. The refinement stage contains 4 Transformer blocks. For DeblurDiNAT-L, one more residual block is appended to each encoder; the number of Transformer blocks increment to [6, 12, 18]. We trained both models using Adam optimizer with the initial learning rate of 10^{-4} which was gradually decayed to 10^{-7} by the cosine annealing strategy. The batch size was set to 8. We augmented input data using random cropping, flipping and rotation. We pre-trained DeblurDiNAT models for 3000 epochs with a patch size of 256×256 and further trained them for another 1000 epochs with a patch size of 512×512 . DeblurDiNAT was trained on eight NVIDIA A100 GPUs.

4.2 Performance Comparison

Quantitative Analysis We compare DeblurDiNAT with existing SOTA deblurring models, including CNNs [5, 11, 25, 32, 33, 38, 48] and Transformers [23, 40, 42, 47]. All models were only trained on the GoPro dataset and tested on the GoPro [33], HIDE [36], RealBlur-R [35] and RealBlur-J [35] datasets. The image quality metrics PSNR/SSIM, and inference time are tested with full resolution 1280×720 images on a single NVIDIA A100 GPU. The number of FLOPs and GPU consumption are calculated with an input tensor of size 256×256 on an NVIDIA 3090 GPU. The GPU consumption is computed by the “torch.cuda.max memory allocated” function.

Tab. 1 shows that our proposed DeblurDiNAT-L holds the second position in the PSNR score rankings, following FFTformer [23], on the two synthetic datasets GoPro [33] and HIDE [36]. Tab. 2 compares the efficiency of our model to existing deblurring Transformers [23, 40, 42, 47]. It reports that DeblurDiNAT-L has 61% less GPU memory consumption and runs $3.21 \times$ faster than FFTformer [23] which heavily involves complex matrix operations. Qualitative analysis (see Sec. 4.2) presents that our restored images are visually closer to the clean images than those of FFTformer [23]. DeblurDiNAT-S achieves satisfactory deblurring quality, which is comparable to the best CNN-based deblurring model MPRNet [32], while with 87% fewer FLOPs and 53% less inference time, as shown in Tab. 2. The PSNR scores of DeblurDiNAT-L measured on the RealBlur-J and RealBlur-R datasets [35] are higher than those of CNNs. Compared to

Table 1: Quantitative evaluations on the GoPro [33], HIDE [36], RealBlur-R [35] and RealBlur-J [35] datasets. The best, second-best and third-best PSNR scores are **highlighted**, underlined and double-underlined. The average PSNR is calculated over the four datasets with equal weights to measure model robustness quantitatively.

Method	GoPro		HIDE		RealBlur-R		RealBlur-J		Avg.
	PSNR	SSIM	PSNR	SSIM	PSNR	SSIM	PSNR	SSIM	PSNR
Nah <i>et al.</i> [33]	29.08	0.914	25.73	0.874	32.51	0.841	27.87	0.827	28.80
DeblurGAN-v2 [25]	29.55	0.934	26.61	0.875	35.26	0.944	28.70	0.866	30.03
SRN [38]	30.26	0.934	28.36	0.915	35.66	0.947	28.56	0.867	30.71
DSD [11]	30.90	0.935	29.11	0.913	-	-	-	-	-
DMPHN [48]	31.20	0.940	29.09	0.924	35.70	0.948	28.42	0.860	31.10
MIMO-UNet+ [5]	32.45	0.957	29.99	0.930	35.54	0.947	27.63	0.837	31.40
MPRNet [32]	32.66	0.959	30.96	0.939	35.99	0.952	28.70	0.873	32.08
Restormer [47]	32.92	0.961	<u>31.22</u>	0.942	36.19	0.957	<u>28.96</u>	0.879	<u>32.32</u>
Uformer-B [42]	33.06	0.967	30.90	0.953	36.19	0.956	29.09	0.886	32.31
Stripformer [40]	<u>33.08</u>	0.962	31.03	0.940	<u>36.08</u>	0.954	28.82	0.876	32.25
FFTformer [23]	34.21	0.969	31.62	0.946	35.87	0.953	27.75	0.853	<u>32.36</u>
DeblurDiNAT-S	32.85	0.961	30.65	0.936	35.92	0.954	28.80	0.877	32.06
DeblurDiNAT-L	<u>33.42</u>	0.965	<u>31.28</u>	0.943	<u>36.07</u>	0.956	<u>28.99</u>	0.885	32.44

Uformer-B [42] with the highest PSNR on RealBlur [35], our DeblurDiNAT-L also demonstrates competitive image quality scores and runs $4.49\times$ faster with 68% fewer parameters. Importantly, Tab. 1 reports that DeblurDiNAT-L obtains an average boost of 0.08 dB over the previous best approach FFTformer [23], which proves that our method demonstrates the strongest generalization ability. From Tab. 1 and Tab. 2, we argue that our DeblurDiNAT guarantees efficacy, efficiency and robustness quantitatively.

Qualitative Analysis The PSNR/SSIM metrics may not precisely measure the visual quality of deblurred images as perceived by human eyes. In this section, we present that the deblurred images produced by DeblurDiNAT-L stand out for their superior visual quality on both synthetic and real-world datasets [33,35,36]. All deblurring models are trained only on GoPro [33]. PSNR values are calculated based on the full-size images. Fig. 4 and Fig. 5 show that our method produces cleaner plate numbers and vivid facial details. Comparing a vast number of deblurred images using human eyes, we also notice that our DeblurDiNAT-L demonstrates a stronger generalization ability over existing models. For example, Fig. 6 shows that FFTformer [23] with the highest PSNR score tested on GoPro introduces unpleasant color changes when applied to the RealBlur-J dataset [35]; Uformer-B [42] with the best quantitative results on RealBlur datasets [35] might distort the appearance of texts according to our experiments. However, ours not only successfully preserves original picture colors but also clearly restores local details and structures of objects with real-world blur artifacts. Fig. 7 shows

Table 2: Model efficiency comparisons based on parameters, FLOPs, inference time, and GPU consumption.

Method	Params (M)	FLOPs (G)	Time (ms)	GPU Mem. (GB)
MIMO-Unet+ [5]	<u>16.1</u>	154.41	47.1	1.4
MPRNet [32]	20.1	777.01	46.3	5.8
Restormer [47]	26.1	<u>140.99</u>	<u>21.00</u>	11.8
Uformer-B [42]	50.9	85.72	676.1	<u>3.4</u>
Stripformer [40]	19.7	170.46	20.0	<u>3.0</u>
FFTformer [23]	<u>16.6</u>	-	483.8	19.0
DeblurDiNAT-S	9.1	<u>99.46</u>	<u>21.7</u>	4.7
DeblurDiNAT-L	<u>16.1</u>	152.61	150.5	7.4

**Fig. 4:** Qualitative comparisons on the GoPro dataset [33].

that DeblurDiNAT-L generates tidy texts and colorful graphic symbols from a blurry image in low-light environments, where the other networks fall short (feel free to zoom images in and out). From the above comparisons, we assert that DeblurDiNAT-L generates deblurred images with the best overall visual quality. More visual results are provided in supplementary materials.

4.3 Ablation Study

In this section, we conduct ablation experiments to evaluate each component of DeblurDiNAT on the GoPro dataset [33]. We trained all models on two NVIDIA A100 GPUs with a patch size of 128×128 for 3000 epochs only. The test settings are the same as the ones in Sec. 4.2.

Effect of ADFS Alternating Dilation Factor Structure (ADFS) is essentially a global-local attention strategy. CMSA enhances the learning of more local representations by decreasing the dilation factor, allowing to capture region-specific blurred patterns. Using local CMSA and global CMSA alternately obtains gains of 0.25 dB over the network with only local CMSA and 0.02 dB compared to



Fig. 5: Qualitative comparisons on the HIDE dataset [36].

Table 3: Investigation on Alternating Dilation Factor Structure.

Local or global	PSNR/SSIM	Params (M)	FLOPs (G)	Time (ms)
only local	31.73/0.951	9.082	99.41	19.6
only global	31.96/0.953	9.082	99.41	20.3
local+global	31.98/0.953	9.082	99.41	19.7

the architecture with only global CMSA (see Tab. 3). It is worth mentioning that such an alternating method adds very few computational costs and only increases the inference time by 0.51%.

Effect of LGFF We design LGFF as a multi-scale feature fusion module, while further experiments in Tab. 4 show that it is also suitable for same-scale features. Fig. 3 compares the structures of several fusion units. In Tab. 4, replacing AFF [5] by LGFF (enhanced with SA) yields the same quality scores with 27 thousands fewer parameters and 0.6 G fewer FLOPs. Removing the SA layers from LGFF does no harm to PSNR and SSIM results, and brings about greater model efficiency, as shown in the third and fourth rows of Tab. 4. It also presents

Table 4: Comparisons among combinations of different feature fusion methods. The component column is multi-scale fusion + same-scale fusion.

Network	Component	PSNR/SSIM	Params (M)	FLOPs (G)
Feature fusion	AFF [5]+SFF	31.88/0.953	9.123	100.31
	LGFF(SA=True)+SFF	31.88/0.953	9.096	99.71
	LGFF(SA=True)+GFN	31.89/0.953	9.079	99.28
	LGFF+GFN	31.89/0.953	8.995	97.13
	LGFF+LGFF	31.96/0.953	9.082	99.41

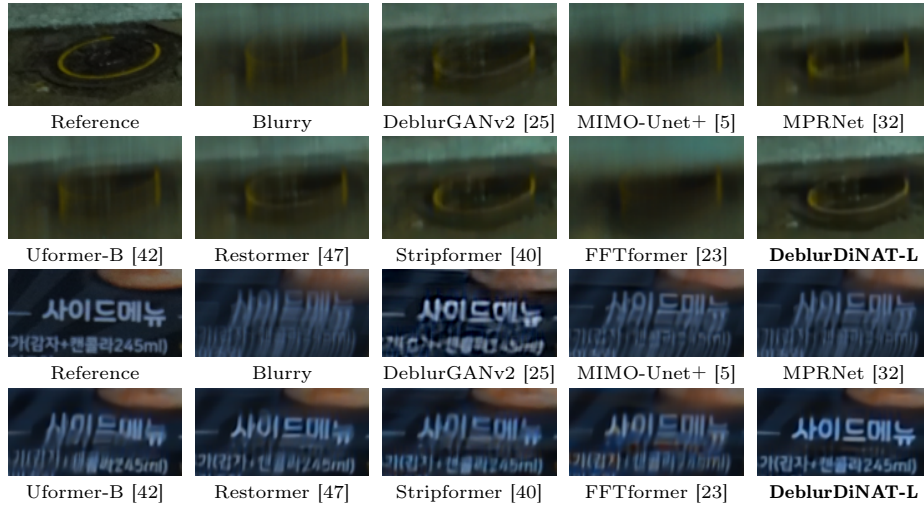


Fig. 6: Qualitative comparisons on the RealBlur-J dataset [35].



Fig. 7: Qualitative comparisons on the RealBlur-R dataset [35].

that applying LGFF to both multi-scale and same-scale feature fusion provides an overall gain of 0.08 dB and improved efficiency over the baseline.

Effect of CCL We investigate how different positions of cross-channel learner (CCL) in CMSA and various pooling strategies used in CCL affect deblurring performance. Tab. 5 shows that, our parallel design obtains a 0.08 dB gain and 2.26% speedup over the strategy placing CCL before the self-attention blocks. The global average pooling (GAP) in CCL leads to 0.18 dB boost over the global max pooling (GMP). Compared to the self-attention without channel modulation, our proposed CMSA improves PSNR by 0.09 dB.

Effect of DMFN Experiment data in Tab. 5 demonstrates that our straightforward DMFN brings a performance improvement of 0.07 dB PSNR compared

Table 5: Influence of CCL and DMFN. In the CCL group, the positions of CCL and impacts of different global pooling methods are investigated.

Network	Component	PSNR/SSIM	FLOPs (G)	Time (ms)
CCL	CMSA w/o CCL	31.98/0.953	99.41	19.7
	CCL before SA+GAP	31.99/0.954	99.46	22.6
	CCL after SA+GAP	32.01/0.954	99.46	22.2
	parallel+GMP	31.89/0.952	99.46	21.7
	parallel+GAP	32.07/0.954	99.46	22.1
Feed-forward	GDFN [47]	31.98/0.953	99.41	19.7
	DMFN	32.05/0.954	99.41	19.4

Table 6: Comparison experiments among different self-attention mechanisms.

self-attention	PSNR	Params (M)	FLOPs (G)	Time (ms)	GPU Mem. (GB)
Restormer [47]	30.76	<u>9.141</u>	<u>100.88</u>	18.0	<u>5.23</u>
Stripformer [40]	<u>31.21</u>	8.776	97.19	64.2	<u>5.90</u>
FFTformer [23]	<u>32.04</u>	11.872	125.98	<u>54.1</u>	<u>9.30</u>
CMSA	32.07	<u>9.082</u>	<u>99.46</u>	<u>22.1</u>	4.73

to GDFN [47] with gating mechanisms. Although both of them share similar numbers of FLOPs, GDFN offers a 1.5% speedup.

Analysis on Self Attention We compare CMSA with self-attention mechanisms used in Restormer [47], Stripformer [40] and FFTformer [23], three SOTA Transformers designed for image deblurring. We replace the self-attention modules CMSA in DeblurDiNAT with theirs. As reported in Tab. 6, ours outperforms the other attention methods in terms of PSNR and GPU memory consumption. Compared to SA employed in FFTformer [23], ours achieves 0.03 dB higher PSNR, 2.45 \times faster speed and 49% less GPU memory consumption.

5 Conclusion

In this work, we proposed a novel Transformer, called DeblurDiNAT, and introduced four key designs to solve existing issues of deblurring Transformers. Firstly, an alternating dilation factor structure is utilized to recognize both local and global blurred patterns. Then, DeblurDiNAT uses a cross-channel learner to modulate the self-attention outputs dynamically, so that cross-channel interactions can be learnt from complex image data. With the aim of efficient feature propagation, a divide and multiply feed-forward network replaces the conventional approach composed of fully connected layers and activation functions. In addition, a lightweight gated feature fusion method is created to aggregate multi-scale or same-scale features. Comprehensive experiments demonstrate that our

architecture outperforms SOTA models in regard to the efficiency and efficacy balance, and ours exhibits the strongest generalization ability.

References

1. Bahat, Y., Efrat, N., Irani, M.: Non-uniform blind deblurring by reblurring. In: Proceedings of the IEEE international conference on computer vision. pp. 3286–3294 (2017)
2. Biemond, J., Lagendijk, R.L., Mersereau, R.M.: Iterative methods for image deblurring. Proceedings of the IEEE **78**(5), 856–883 (1990)
3. Chen, X., He, X., Yang, J., Wu, Q.: An effective document image deblurring algorithm. In: CVPR 2011. pp. 369–376. IEEE (2011)
4. Cho, H., Wang, J., Lee, S.: Text image deblurring using text-specific properties. In: Computer Vision–ECCV 2012: 12th European Conference on Computer Vision, Florence, Italy, October 7–13, 2012, Proceedings, Part V 12. pp. 524–537. Springer (2012)
5. Cho, S.J., Ji, S.W., Hong, J.P., Jung, S.W., Ko, S.J.: Rethinking coarse-to-fine approach in single image deblurring. In: Proceedings of the IEEE/CVF international conference on computer vision. pp. 4641–4650 (2021)
6. Dai, Y., Gieseke, F., Oehmcke, S., Wu, Y., Barnard, K.: Attentional feature fusion. In: Proceedings of the IEEE/CVF winter conference on applications of computer vision. pp. 3560–3569 (2021)
7. Dong, C., Loy, C.C., He, K., Tang, X.: Learning a deep convolutional network for image super-resolution. In: Computer Vision–ECCV 2014: 13th European Conference, Zurich, Switzerland, September 6–12, 2014, Proceedings, Part IV 13. pp. 184–199. Springer (2014)
8. Dong, H., Pan, J., Xiang, L., Hu, Z., Zhang, X., Wang, F., Yang, M.H.: Multi-scale boosted dehazing network with dense feature fusion. In: Proceedings of the IEEE/CVF conference on computer vision and pattern recognition. pp. 2157–2167 (2020)
9. Dosovitskiy, A., Beyer, L., Kolesnikov, A., Weissenborn, D., Zhai, X., Unterthiner, T., Dehghani, M., Minderer, M., Heigold, G., Gelly, S., et al.: An image is worth 16x16 words: Transformers for image recognition at scale. arXiv preprint arXiv:2010.11929 (2020)
10. Fu, Z., Zheng, Y., Ma, T., Ye, H., Yang, J., He, L.: Edge-aware deep image deblurring. Neurocomputing **502**, 37–47 (2022)
11. Gao, H., Tao, X., Shen, X., Jia, J.: Dynamic scene deblurring with parameter selective sharing and nested skip connections. In: Proceedings of the IEEE/CVF conference on computer vision and pattern recognition. pp. 3848–3856 (2019)
12. Gupta, A., Joshi, N., Lawrence Zitnick, C., Cohen, M., Curless, B.: Single image deblurring using motion density functions. In: Computer Vision–ECCV 2010: 11th European Conference on Computer Vision, Heraklion, Crete, Greece, September 5–11, 2010, Proceedings, Part I 11. pp. 171–184. Springer (2010)
13. Han, K., Wang, Y., Chen, H., Chen, X., Guo, J., Liu, Z., Tang, Y., Xiao, A., Xu, C., Xu, Y., et al.: A survey on vision transformer. IEEE transactions on pattern analysis and machine intelligence **45**(1), 87–110 (2022)
14. Hassani, A., Shi, H.: Dilated neighborhood attention transformer. arXiv preprint arXiv:2209.15001 (2022)

15. Hassani, A., Walton, S., Li, J., Li, S., Shi, H.: Neighborhood attention transformer. In: Proceedings of the IEEE/CVF Conference on Computer Vision and Pattern Recognition. pp. 6185–6194 (2023)
16. Hendrycks, D., Gimpel, K.: Gaussian error linear units (gelus). arXiv preprint arXiv:1606.08415 (2016)
17. Hirsch, M., Schuler, C.J., Harmeling, S., Schölkopf, B.: Fast removal of non-uniform camera shake. In: 2011 International Conference on Computer Vision. pp. 463–470. IEEE (2011)
18. Hradiš, M., Kotera, J., Zemčík, P., Šroubek, F.: Convolutional neural networks for direct text deblurring. In: Proceedings of BMVC (2015)
19. Hu, J., Shen, L., Sun, G.: Squeeze-and-excitation networks. In: Proceedings of the IEEE conference on computer vision and pattern recognition. pp. 7132–7141 (2018)
20. Hua, Y., Liu, Y., Li, B., Lu, M.: Dilated fully convolutional neural network for depth estimation from a single image. In: 2019 International Conference on Computational Science and Computational Intelligence (CSCI). pp. 612–616. IEEE (2019)
21. Ji, S.W., Lee, J., Kim, S.W., Hong, J.P., Baek, S.J., Jung, S.W., Ko, S.J.: Xydeblur: divide and conquer for single image deblurring. In: Proceedings of the IEEE/CVF Conference on Computer Vision and Pattern Recognition. pp. 17421–17430 (2022)
22. Jiang, Y., Chang, S., Wang, Z.: Transgan: Two transformers can make one strong gan. arXiv preprint arXiv:2102.07074 1(3) (2021)
23. Kong, L., Dong, J., Ge, J., Li, M., Pan, J.: Efficient frequency domain-based transformers for high-quality image deblurring. In: Proceedings of the IEEE/CVF Conference on Computer Vision and Pattern Recognition. pp. 5886–5895 (2023)
24. Kupyn, O., Budzan, V., Mykhailych, M., Mishkin, D., Matas, J.: Deblurgan: Blind motion deblurring using conditional adversarial networks. In: Proceedings of the IEEE conference on computer vision and pattern recognition. pp. 8183–8192 (2018)
25. Kupyn, O., Martyniuk, T., Wu, J., Wang, Z.: Deblurgan-v2: Deblurring (orders-of-magnitude) faster and better. In: Proceedings of the IEEE/CVF international conference on computer vision. pp. 8878–8887 (2019)
26. Li, B., Hua, Y., Lu, M.: Advanced multiple linear regression based dark channel prior applied on dehazing image and generating synthetic haze. arXiv preprint arXiv:2103.07065 (2021)
27. Li, B., Zhang, W., Lu, M.: Multiple linear regression haze-removal model based on dark channel prior. In: 2018 International Conference on Computational Science and Computational Intelligence (CSCI). pp. 307–312. IEEE (2018)
28. Li, X., Zhao, H., Han, L., Tong, Y., Tan, S., Yang, K.: Gated fully fusion for semantic segmentation. In: Proceedings of the AAAI conference on artificial intelligence. pp. 11418–11425 (2020)
29. Liu, H., Li, B., Lu, M., Wu, Y.: Real-world image deblurring via unsupervised domain adaptation. In: International Symposium on Visual Computing. pp. 148–159. Springer (2023)
30. Liu, Z., Lin, Y., Cao, Y., Hu, H., Wei, Y., Zhang, Z., Lin, S., Guo, B.: Swin transformer: Hierarchical vision transformer using shifted windows. In: Proceedings of the IEEE/CVF international conference on computer vision. pp. 10012–10022 (2021)
31. Lu, Q., Zhou, W., Fang, L., Li, H.: Robust blur kernel estimation for license plate images from fast moving vehicles. IEEE transactions on image processing 25(5), 2311–2323 (2016)

32. Mehri, A., Ardakani, P.B., Sappa, A.D.: Mprnet: Multi-path residual network for lightweight image super resolution. In: Proceedings of the IEEE/CVF Winter Conference on Applications of Computer Vision. pp. 2704–2713 (2021)
33. Nah, S., Hyun Kim, T., Mu Lee, K.: Deep multi-scale convolutional neural network for dynamic scene deblurring. In: Proceedings of the IEEE conference on computer vision and pattern recognition. pp. 3883–3891 (2017)
34. Purohit, K., Rajagopalan, A.: Region-adaptive dense network for efficient motion deblurring. In: Proceedings of the AAAI Conference on Artificial Intelligence. pp. 11882–11889 (2020)
35. Rim, J., Lee, H., Won, J., Cho, S.: Real-world blur dataset for learning and benchmarking deblurring algorithms. In: Computer Vision–ECCV 2020: 16th European Conference, Glasgow, UK, August 23–28, 2020, Proceedings, Part XXV 16. pp. 184–201. Springer (2020)
36. Shen, Z., Wang, W., Lu, X., Shen, J., Ling, H., Xu, T., Shao, L.: Human-aware motion deblurring. In: Proceedings of the IEEE/CVF International Conference on Computer Vision. pp. 5572–5581 (2019)
37. Svoboda, P., Hradiš, M., Maršík, L., Zemčík, P.: Cnn for license plate motion deblurring. In: 2016 IEEE International Conference on Image Processing (ICIP). pp. 3832–3836. IEEE (2016)
38. Tao, X., Gao, H., Shen, X., Wang, J., Jia, J.: Scale-recurrent network for deep image deblurring. In: Proceedings of the IEEE conference on computer vision and pattern recognition. pp. 8174–8182 (2018)
39. Tran, P., Tran, A.T., Phung, Q., Hoai, M.: Explore image deblurring via encoded blur kernel space. In: Proceedings of the IEEE/CVF Conference on Computer Vision and Pattern Recognition. pp. 11956–11965 (2021)
40. Tsai, F.J., Peng, Y.T., Lin, Y.Y., Tsai, C.C., Lin, C.W.: Stripformer: Strip transformer for fast image deblurring. In: European Conference on Computer Vision. pp. 146–162. Springer (2022)
41. Vaswani, A., Shazeer, N., Parmar, N., Uszkoreit, J., Jones, L., Gomez, A.N., Kaiser, Ł., Polosukhin, I.: Attention is all you need. *Advances in neural information processing systems* **30** (2017)
42. Wang, Z., Cun, X., Bao, J., Zhou, W., Liu, J., Li, H.: Uformer: A general u-shaped transformer for image restoration. In: Proceedings of the IEEE/CVF conference on computer vision and pattern recognition. pp. 17683–17693 (2022)
43. Xu, L., Jia, J.: Two-phase kernel estimation for robust motion deblurring. In: Computer Vision–ECCV 2010: 11th European Conference on Computer Vision, Heraklion, Crete, Greece, September 5–11, 2010, Proceedings, Part I 11. pp. 157–170. Springer (2010)
44. Yan, Y., Ren, W., Guo, Y., Wang, R., Cao, X.: Image deblurring via extreme channels prior. In: Proceedings of the IEEE Conference on Computer Vision and Pattern Recognition. pp. 4003–4011 (2017)
45. Yu, F., Koltun, V.: Multi-scale context aggregation by dilated convolutions. arXiv preprint arXiv:1511.07122 (2015)
46. Yuan, L., Chen, Y., Wang, T., Yu, W., Shi, Y., Jiang, Z.H., Tay, F.E., Feng, J., Yan, S.: Tokens-to-token vit: Training vision transformers from scratch on imagenet. In: Proceedings of the IEEE/CVF international conference on computer vision. pp. 558–567 (2021)
47. Zamir, S.W., Arora, A., Khan, S., Hayat, M., Khan, F.S., Yang, M.H.: Restormer: Efficient transformer for high-resolution image restoration. In: Proceedings of the IEEE/CVF conference on computer vision and pattern recognition. pp. 5728–5739 (2022)

48. Zhang, H., Dai, Y., Li, H., Koniusz, P.: Deep stacked hierarchical multi-patch network for image deblurring. In: Proceedings of the IEEE/CVF Conference on Computer Vision and Pattern Recognition. pp. 5978–5986 (2019)
49. Zhang, K., Zuo, W., Zhang, L.: Learning a single convolutional super-resolution network for multiple degradations. In: Proceedings of the IEEE conference on computer vision and pattern recognition. pp. 3262–3271 (2018)
50. Zhang, K., Ren, W., Luo, W., Lai, W.S., Stenger, B., Yang, M.H., Li, H.: Deep image deblurring: A survey. *International Journal of Computer Vision* **130**(9), 2103–2130 (2022)
51. Zou, W., Jiang, M., Zhang, Y., Chen, L., Lu, Z., Wu, Y.: Sdwnet: A straight dilated network with wavelet transformation for image deblurring. In: Proceedings of the IEEE/CVF international conference on computer vision. pp. 1895–1904 (2021)